Multiple junction biasing of superconducting tunnel junction detectors

K. Segall
Department of Physics and Astronomy, Colgate University, Hamilton, New York 13346

J. J. Mazo
Departamento de Física de la Materia Condensada and ICMA, CSIC-Universidad de Zaragoza, 50009 Zaragoza, Spain

T. P. Orlando
Department of Electrical Engineering and Computer Science, Massachusetts Institute of Technology, Cambridge, Massachusetts 02139

(Received 6 October 2004; accepted 8 February 2005; published online 7 April 2005)

We describe a biasing scheme for single-photon detectors based on superconducting tunnel junctions. It replaces a single detector junction with a circuit of three junctions and achieves biasing of a detector junction at subgap currents without the use of an external magnetic field. This potentially increases the capability of these types of detectors and eases constraints in making large arrays. The biasing occurs through the nonlinear interaction of the three junctions, which we demonstrate through numerical simulation. This nonlinear state is numerically stable against external fluctuations and is compatible with high-fidelity electrical readout of the photon-induced current. © *2005 American Institute of Physics*. [DOI: 10.1063/1.1890467]

Over the past two decades, the use of single-photon detectors based on superconducting tunnel junctions (STJs) has received considerable attention.[1] In these detectors, a photon with energy larger than the superconducting energy gap is absorbed in a STJ, creating quasiparticle excitations. These quasiparticles can be read out as a current pulse through the STJ. The integrated charge from this pulse can be used as a measure of the photon energy, giving the detectors inherent spectral resolving power. Besides the energy resolution, these detectors also offer single-photon efficiency and a large absorption count rate.

In order to operate properly, the STJ detector must be biased at a voltage between zero and $(2\Delta/e)$, where 2Δ is the energy gap of the superconductor and e is the electron charge. This range is known as the subgap region. To bias stably in the subgap region, a small magnetic field is usually applied parallel to the junction in order to suppress the Josephson supercurrent. A stable bias without a magnetic field is theoretically possible, but in practice usually results in significant signal reduction and/or added noise in the photon pulse readout.[2] While the application of a parallel field is not difficult, it can be limiting for certain applications. For example, single-photon detectors based on a competing technology, the transition-edge sensor (TES), are used successfully in microanalysis applications involving a scanning electron microscope (SEM).[3] A SEM is used to locally excite a sample of interest, while a TES detector measures the spectroscopic composition of the luminescent x-ray photons, allowing identification of the host material. STJ detectors, which are competitive with TES detectors in other fields, are not as feasible for this application, since the applied magnetic field deflects the electron beam, necessitating large sample–detector spacing. Removing the need for a magnetic field could thus open up new applications for the STJ detector. In addition, in scaling to larger arrays of STJ detectors, the magnetic field suppression of the supercurrent can become difficult. Small differences in junction fabrication may necessitate a slightly different field for each junction, requiring a separate electrical lead for each junction. Removing the need for a magnetic field is thus an attractive option.

In this letter we propose a new biasing scheme for a STJ detector based on a circuit of multiple junctions which removes the need for a magnetic field. The biasing occurs through the nonlinear interaction of the detector junction(s) with other junctions in the circuit. This nonlinear state can only be obtained with multiple junctions and not with resistors. The circuit is still compatible with high-fidelity pulse readout, and the bias voltage is numerically stable against external fluctuations. Here we describe the circuit concept, show simulations to demonstrate its operation, and discuss practical considerations for detector designs.

The proposed circuit is shown in Fig. 1. The detector junction (junction 3) is placed in series with a second junction (junction 2) and then both are placed in parallel with a third junction (junction 1). The ratio of the critical currents is 1, 0.5, and 0.5 for junctions 1, 2, and 3, respectively; other combinations are possible. A current (I_T) is applied to the three junctions as shown. Figure 2(a) shows how to reach desired operating state. First the current I_T is increased until all three junctions have switched into the finite voltage state. Then the current is reduced to approximately the operating current shown in Fig. 2(a). Summing the voltages around the loop requires that $V_1=V_2+V_3$. In the desired state, junction 1 is biased at the superconducting energy gap $(V_1=V_g=2\Delta/e)$ and junctions 2 and 3 are biased at half the energy

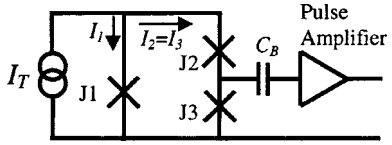

FIG. 1. Circuit schematic for magnetic-field free detector biasing. The X's represent junctions. Applied current I_T splits between the two branches; the same current flows through junctions 2 and 3. The pulse amplifier is shown AC coupled to junction 3. Photon-excited quasiparticles can be read out through junctions 2, 3, or both.

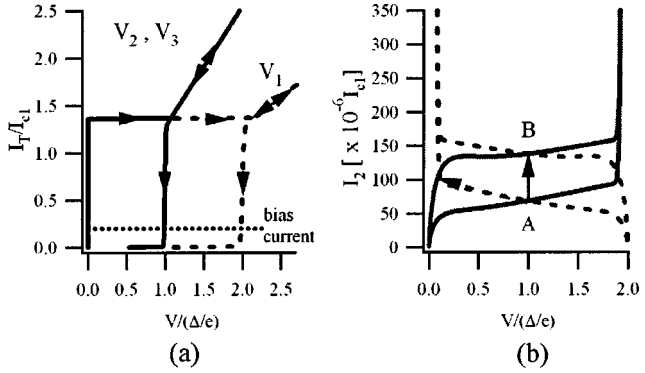

FIG. 2. (a) Hysteretic dynamics for the circuit shown in Fig. 1. I_T is plotted against the voltage for junctions 1 (dotted line), 2, and 3 (both solid lines). I_T is initially increased until the three junctions switch to nonzero voltage; then the current is decreased. At the bias current, junctions 2 and 3 are in the subgap region where they can function as photon detectors; here nearly all the current I_T is flowing through junction 1. (b) I-V curves showing the subgap current for junctions 2 and 3. $I_2=I_3$ is plotted versus V_3, solid line, and (V_g-V_3) dotted line. The two lower curves are for a temperature $(kT/\Delta=1/9)$ and the two upper curves are for $(kT/\Delta=1/8)$. At the lower temperature, the intersection of the two curves gives the operating point. The heat from a photon coupled to both junctions causes the system to move from A to B, straight up. Heat only coupled to one of the junctions causes it to move to the left.

gap $(V_2=V_3=V_g/2)$. At this point junctions 2 and/or 3 can function as a detector; no magnetic field has been applied.[4]

We first show nonlinear simulations of the biasing state and then discuss practical considerations for detector design. To simulate the circuit, we solve the usual RSJ model[5] for each junction with an added term for the subgap current. The normalized current through junction j is given by

$$i_j = h_j\left(\frac{d^2\varphi_j}{d\tau^2} + \Gamma(\nu_j)\frac{d\varphi_j}{d\tau} + \sin\varphi_j + i_{ss}(\nu_j)\right), \tag{1}$$

where φ is the phase difference across a given junction, ν is its normalized voltage $(\nu=d\varphi/d\tau)$, $\tau=\omega_p t$ is the normalized time, ω_p is the plasma frequency, t is time, $\Gamma(\nu)$ is the voltage-dependent damping, h is the anisotropy parameter for the size of the different junctions, and i_{ss} is the voltage-dependent subgap current. The subscript j runs over the three junctions in the circuit. The currents i_j are normalized to the critical current of the first junction, I_{c1}. The plasma frequency ω_p is given by $\omega_p^2=2\pi I_c/\Phi_0 C$, where Φ_0 is the flux quantum and C is the junction capacitance. The theoretical BCS subgap current, i_{ss}, depends exponentially on temperature and is given in Ref. 6. The nonlinear damping parameter Γ is given by $\Gamma=\Gamma_N g(\nu)$, where Γ_N is the damping in the normal state, given by $\Gamma_N^2=\Phi_0/2\pi I_C R_N^2 C$, and $g(\nu)$ is the voltage-dependent damping. To account for the damping in the subgap region and for the gap rise, we use the following empirical form for $g(\nu)$:[7]

$$g(\nu) = g_{sg} + \frac{1-g_{sg}}{2}\left\{1-\tanh\left[100\left(1-\frac{\nu_j}{\nu_g}\right)\right]\right\}, \tag{2}$$

where g_{sg} is a constant damping in the subgap region and ν_g is the normalized gap voltage. Equation (2) gives $\Gamma(\nu)=g_{sg}\Gamma_N$ for $V<(2\Delta/e)$ and $\Gamma(\nu)=\Gamma_N$ for $V>(2\Delta/e)$.

To write the equations of the circuit we use fluxoid quantization and current conservation. Fluxoid quantization gives $(\varphi_1-\varphi_2-\varphi_3)=2\pi f_{\rm ind}$, where $f_{\rm ind}$ is the induced frustration in the loop formed by the three junctions. Current conservation gives $i_1=i/2-i_m$ and $i_2=i_3=i/2+i_m$; here i_j is given by Eq. (1), $i=i_1+i_2$, and i_m, the mesh current, is related with $f_{\rm ind}$ through $i_m=2\pi\lambda f_{\rm ind}$. The parameter $\lambda=\Phi_0/(2\pi L I_{c1})$ measures the importance of induced fields; L is the geometric inductance of the loop.[8]

The results of the model are shown in Fig. 2(a). The parameters used are $\Gamma_N=0.02$, $h_1=1$, $h_2=0.5$, $h_3=0.5$, $g_{sg}=10^{-4}$, and $\lambda=10$. Initially, as I_T is increased, all three junctions are in the zero-voltage state. At a current of approximately $I_T=1.3I_{c1}$ the system switches to a running mode, where $V_1=V_g$ and $V_2=V_3=(V_g/2)$. In real experiments the switching of the three junctions is affected by fluctuations, which are not included in Fig. 2(a). In any case, for reaching a detector biasing point, these switching dynamics are unimportant; one simply increases the current to a value large enough to ensure that all three junctions have switched. Once this point has been reached, the current is then decreased to the operating current shown, approximately $I_T=0.2I_{c1}$. Operating currents as large as $I_T=0.5I_{c1}$ give stable dynamics, but for noise purposes lower values of I_T are more desirable. Following this procedure ensures the desired state will be obtained. If the current is decreased further, the system will retrap to the zero voltage state across all three junctions. Figure 2(a) plots the *total* current I_T on the y axis; at the operating point shown, nearly *all* of this current I_T is flowing though junction 1. Only the small subgap current flows through junctions 2 and 3. This subgap current for two different temperatures is shown by the solid lines in Fig. 2(b); they resemble a typical STJ I–V curve.

This state of the detector was motivated by a type of nonlinear dynamical state in a Josephson array called a breather, which is an intrinsically localized mode that exists in a ladder array driven by a uniform current.[9] The so-called type B breather has a similar voltage pattern of V_g, $V_g/2$, and $V_g/2$ for three junctions around a loop. Although not identical, the circuit in Fig. 1 has similar hysteretic dynamics to the type B breather state. We have found that other nonlinear states coexist in the circuit with the desired state. We studied the stability of the detector state against external fluctuations by adding a noise term to each junction in Eq. (1), and find stability for times orders of magnitude longer than typical experimental times.

The main fabrication requirement for reaching this biasing state is that the junctions be highly underdamped. Values of $\Gamma_N<0.05$ result in the ideal dynamics that are shown in Fig. 2(a) and 2(b). For $0.1>\Gamma_N>0.05$, the nonlinear biasing state still exists, but with an increased dc current through junctions 2 and 3, which will result in some excess noise. For $\Gamma_N>0.1$, the dynamics becomes more complicated than we have shown in Fig. 2(a) and 2(b). For niobium (Nb) junctions, achieving $\Gamma_N<0.05$ requires fabricating a current density (J_c) of about 200 $\mathrm{A/cm^2}$ or less, which is satisfied by most detector junctions tested to date. For aluminum (Al) junctions the current density should be lower, around $J_c \sim 5\ \mathrm{A/cm^2}$. This is achievable in most fabrication processes, although many Al junctions tested to date have values of J_c slightly higher, around 30 $\mathrm{A/cm^2}$. The loop inductance parameter, λ, appears to have no major constraints.[10] We comment more on the possible circuit parameters in a future paper.[11]

With the circuit biased at the desired operating point, away from the hysteresis and switching in Fig. 2(a), a simpler dc model can be used to predict currents and voltages at

the operating point of the circuit with the same accuracy as the full model. These results can be used to show the operation of the detector in response to an absorbed photon and to discuss issues of impedance and noise. In the dc model, we change Eq. (1) to $i_j = h_j[\Gamma(v_j)v_j + i_{ss}(v_j)]$ and keep the relations $V_1 = V_2 + V_3$; $i_2(V_2) = i_3(V_3)$; and $i = i_1(V_1) + i_2(V_2)$, defining a system of algebraic equations which can be numerically solved. At the operating point $V_1 = V_g$ and $V_2 = (V_g - V_3)$. We can then solve the dc model equations graphically by plotting $I_3 = I_2$ vs V_2 and versus $(V_g - V_3)$ The intersection gives the operating point of the circuit, as shown in Fig. 2(b).

To simulate the response to a photon, we increase the temperature of the detector junction. In a real detector the temperature first increases, as the excess quasiparticles tunnel through the junction, and then decreases, as the quasiparticles either recombine or diffuse away from the barrier. The detector junction(s) can be junction 2, junction 3, or both. The temperature of junction 1 stays constant. In Fig. 2(b) we show how the operating point can be followed as the subgap current increases. In the case of heating both junctions 2 and 3, the operating point moves straight up from A to B, and then back down from B to A. If only junction 3 is used then it moves to the left and up. To read out the excess tunneling current, a current amplifier can be AC coupled in parallel with junction 3, as shown in Fig. 1; the capacitor (C_B) passes signal frequencies and blocks DC currents.

The extra junctions in the circuit will add additional electronic noise to the amplifier which can potentially degrade the energy resolution of the detector. In many cases the additional noise will cause only a small, even negligible change in the total energy resolution. Under some conditions, the cost can be as large as a factor of two in the energy width. The two main sources of electronic noise are (i) the shot noise due to the current flowing through the junctions, and (ii) the voltage noise of the amplifier, which is converted to current noise due to the junction impedance.[12] The shot noise (i) is proportional to the dc current flowing through each junction. The current flowing through junctions 2 and 3 is the same subgap current that usually flows through a single junction; hence there is no increase over the usual shot noise. The extra current flowing in junction 1 will give some additional shot noise; however, since the impedance of junction 1, biased at the energy gap, is many orders of magnitude smaller than the impedance of junctions 2 and 3, this extra noise current will almost exclusively flow through junction 1 and not through junctions 2 and 3. Thus, it will not add significantly to the total shot noise seen by the amplifier. For the voltage noise (ii), the new impedance seen by the amplifier will be approximately junction 2 in parallel with junction 3. If junctions 2 and 3 have the same dynamic resistance, then the new impedance seen by the amplifier will be a factor of two smaller than the impedance of junction 2 or 3 individually. This increases the contribution of the amplifier voltage noise to the total current noise by a factor of two as compared to a single junction. The actual amount of increase in the energy width caused by the increases in electronic noise will depend on the particular detector geometry, photon energy, and junction size. In addition, the bias current I_T can be tuned for optimal noise performance just as the bias current and magnetic field are tuned in existing STJ detectors.

In addition to noise there are other possible considerations for detector design. In our models we have assumed the theoretical BCS subgap current (i_{ss}) along with an additional linear subgap impedance (g_{sg}). In real devices there are often other contributions to the subgap current, including Fiske modes, normal metal tunneling, and multiparticle Andreev reflection. The importance of these issues will need to be determined through experiments and junction fabrication. A few points should be noted, however. The first is that one need not be constrained by the ratio of 1.0, 0.5, and 0.5 for the critical currents of the three junctions. We have seen that several different ratios give subgap biasing, such as 1.0, 0.5, and 0.3. Different ratios will result in different operating voltages in the subgap region, which can be chosen to avoid any known subgap features. In addition, by using the technique we have described, junction shapes will not be as constrained as they are presently. In existing devices, junction shapes are usually "stretched" in order to allow more efficient supercurrent suppression by the external magnetic field. Since the external field is no longer needed, the junctions can be chosen to be any shape. This would help, for example, in avoiding Fiske modes.[13] Finally, since two of the junctions in the circuit can each be used as a detector, there are possibilities to bias a two-junction detector or even a many-pixel array in the future with this technique. This will free up electrical leads and offer more design flexibility.

We thank E. Trìas, D. E. Prober, M. C. Gaidis, S. Friedrich, and L. Frunzio for useful discussions. We acknowledge the FEDER program (BMF2002-00113), NSF (DMR-9988832), and the Colgate Division of Natural Sciences.

[1] J. Mather, Nature (London) **401**, 654 (1999); N. E. Booth and D. J. Goldie, Supercond. Sci. Technol. **9**, 493 (1996).
[2] It is possible to bias a single junction without a magnetic field using a small resistor, but this will then draw the photon-induced current away from the amplifier. Alternately, an active voltage bias can be provided by the signal amplifier; however, real experiments show that, in this case, a magnetic field is still necessary.
[3] D. A. Wollman, S. W. Nam, G. C. Hilton, K. D. Irwin, N. F. Bergren, D. A. Rudman, J. M. Martinis, and D. E. Newbury, J. Microsc. **199**, 37 (2000).
[4] Aluminum tunnel junctions, which are often used for detectors, typically have an increase in DC current at this value of voltage, $V_g/2$. As we state later in the paper, it is straightforward to change the ratio of the three critical currents slightly, which avoids biasing the detector at exactly this subgap feature.
[5] T. P. Orlando and K. A. Delin, *Foundations of Applied Superconductivity* (Addison-Wesley, Reading, MA, 1991).
[6] T. Van-Duzer and C. W. Turner, *Principles of Superconductive Devices and Circuits* (Edward Arnold, London, UK, 1981).
[7] This constant subgap damping adds a linear current to the subgap current in Eq. (1). We chose a value for this subgap damping which adds less about 10% to the BCS subgap value. This was chosen empirically, to try to match a typical experimental I–V curve.
[8] When deriving the equations we have neglected external magnetic fields and have assumed that the left and right branches of the circuit have the same geometrical inductance; the model can be easily adapted to account for these effects.
[9] E. Trias, J. J. Mazo, and T. P. Orlando, Phys. Rev. Lett. **84**, 741 (2000); P. Binder, D. Abraimov, A. V. Ustinov, S. Flach, and Y. Zolotaryuk, Phys. Rev. Lett. **84**, 745 (2000).
[10] Using $\lambda = 0.1$, $\lambda = 1$, or running the simulation in the limit of no induced fields all give similar results.
[11] K. Segall, J. J. Mazo, and T. P. Orlando, IEEE Trans. Appl. Supercond. (to be published).
[12] K. Segall, C. Wilson, L. Frunzio, L.Li, S.Friedrich, M.C.Gaidis, D.E.Prober, and A.E.Szymkowiak, Appl. Phys. Lett. **76**, 3998 (2000).
[13] M. D. Fiske, Rev. Mod. Phys. **36**, 221 (1964).